20th CNS Simulation Symposium, Sept. 7-9, Niagara-on-the-Lake, Ontario, 1997

A GENERALIZED PREDICTION METHOD FOR SINGLE-PHASE PRESSURE DROP IN A STRING OF ALIGNED CANDU-TYPE BUNDLES

L.K.H. Leung* and G. Hotte**

*AECL, Chalk River Laboratories Chalk River, Ontario K0J 1J0
**Hydro-Quebec, 1155, rue Metcalfe, Bureau 880, Montreal, Quebec H3B 2V6

Abstract

A generalized prediction method has been developed to calculate various pressure-drop components over a string of aligned CANDU[1]-type bundles in single-phase flow. The friction factor is evaluated using the Colebrook equation based on the surface roughness. It is modified with two correction factors to account for the geometry effect (i.e., from a tube to a bundle) and the bundle-eccentricity effect. The pressure loss over the bundle junction is assumed to be caused by (a) the flow impact loss on the exposed regions of the endplate, and (b) the separation loss between two planes of rods. The flow-impact loss is determined using a correlation based on the blockage-area ratio, whereas the separation loss is calculated using data obtained from a bundle-separation test. The pressure drop at either the spacer plane or the bearing-pad plane is calculated based on the blockage-area ratio. Modifications have been introduced to account for (a) the rounding of the leading and trailing edges of a spacer, and (b) the 15° offset from the flow direction. The prediction method has been validated using experimental data obtained with several bundle strings. Good agreement with experimental data was observed for both the frictional pressure drop and the local pressure drops over the junction and the spacer planes.

1. INTRODUCTION

An accurate prediction of pressure drop over a string of 37-element bundles is essential for the precise evaluation of the critical channel power (CCP). The single-phase pressure drop must be estimated closely, since it has a strong influence on the two-phase pressure drop (which is usually calculated by multiplying the single-phase pressure drop with a two-phase multiplier). The pressure drop over a string of CANDU-fuel bundles consists of (a) skin-friction loss, (b) momentum loss, and (c) local losses at the junction (primarily caused by the webs, rod misalignment and rod discontinuity), spacer plane (both spacers and bearing pads), and bearing-pad planes. The calculation for pressure drop due to gravity is not required, since CANDU fuel channels are oriented horizontally.

The frictional pressure drop is caused by shear stresses between the coolant and the fuel sheath, and between the coolant and the pressure tube: it depends on surface roughness, geometry and flow conditions. The pressure drop due to acceleration is a measure of momentum change over a control volume. It can be a significant component in a heated channel with boiling. The local pressure drop due to flow obstruction by appendages in a CANDU bundle is affected primarily by the ratio of blockage area to free flow area, and is often expressed as a pressure-loss coefficient.

It is the objective of this study to derive a generalized prediction method for various pressure-drop components over a string of CANDU-type bundles.

---

[1]CANDU-CANada Deuterium Uranium (a registered trademark)

2. A GENERALIZED PREDICTION METHOD FOR PRESSURE DROPS

A large amount of information and prediction methods are available for predicting the frictional pressure drop, particularly for a simple tube. The present methodology is based on the equation for a simple tube, and accounts for the geometric and eccentricity effects using an equivalent-annuli approach. It is applicable for both laminar and turbulent flow. However, only equations for turbulent flow, which are of most general interest, are presented here.

2.1 Single-Phase Pressure Drop due to Friction

The single-phase pressure drop due to friction for a fully developed flow in bundles is calculated using the D'Arcy equation:

$$\Delta P_{fric.} = \frac{f_{bundle}\,\Delta L}{D_{hy}} \frac{G^2}{2\,\rho_l} \tag{1}$$

where f_{bundle} is the friction factor over the bundle segment with no appendage, L is the channel length in metres, G is the mass flux in $kg{\cdot}m^{-2}{\cdot}s^{-1}$, and ρ_l is the liquid density in $kg{\cdot}m^{-3}$. The hydraulic-equivalent diameter for a bundle, D_{hy}, is defined as

$$D_{hy} = \frac{4\,A_f}{\wp_w} \tag{2}$$

where A_f is the flow area in m^2 and $\wp_w$ is the wetted perimeter of the channel in metres.

Courtaud et al. (1966) and Le Tourneau et al. (1957) demonstrated that the friction factor in bundles is affected by the geometry of the channel and Reynolds number. The simple approach based on the hydraulic-equivalent diameter is not applicable for bundle geometries. Rehme (1973) and Malak et al. (1975) introduced corrections to the friction factor for tubes in turbulent flow (with Reynolds numbers larger than $4{\cdot}10^3$) to account for the bundle effect.

In the present study, a generalized equation based on a modification to the predictions for tubes is recommended for calculating the friction factor in bundle geometries. It is expressed as

$$f_{bundle} = K_{bundle}\,K_{ecc.}\,f_{tube} \tag{3}$$

where f_{tube} is the friction factor for an equivalent-diameter tube of the same relative roughness, K_{bundle} is the geometric correction factor, and $K_{ecc.}$ is the correction factor for eccentricity effect. The friction factor for tubes in transition and fully developed turbulent flow is calculated using the Colebrook equation

$$\frac{1}{f_{tube}^{1/2}} = -2\,\log\left(\frac{\varepsilon/D_{hy}}{3.7} + \frac{2.51}{f_{tube}^{1/2}\,Re}\right) \tag{4}$$

where ε is the surface-roughness height in metres. The correction factor, K_{bundle}, accounts for the difference in geometry (i.e., between tubes and bundles), and is based on the prediction method of Idelchik (1994) for annuli (an equivalent-annuli approach). Figure 1 presents the Idelchik correction factor for various inner-to-outer tube-diameter ratios and Reynolds numbers, Re. The Idelchik correction factor is valid for flow in a smooth channel only. In a rough channel, the friction factor is affected only by the relative roughness of the surface (i.e., ε/D_{hy}) for a fully developed turbulent flow, and is independent of

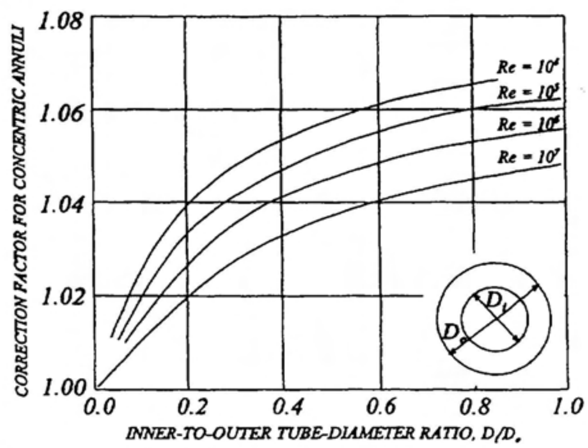

Figure 1: The Idelchik correction factor for annuli.

the Reynolds number. This is the asymptotic trend of the Colebrook equation (Equation (4)). Hence, the correction factor is anticipated to approach an asymptotic value of 1 at high Reynolds numbers. This, however, is not exhibited in the Idelchik correction factor. An empirical modification to the Idelchik correction factor is therefore proposed for turbulent flow

$$K_{bundle} = 1 + (K_{ann,\,Idelchik} - 1)\,\frac{b}{0.311} \qquad (5)$$

The variable, b, is the exponent value in the Blasius-type equation for the rough channel of interest, which is expressed as

$$f = a\,Re^{-b} \qquad (6)$$

The exponent 'b' varies from 0.311 for a smooth tube (based on the Bhatti and Shah (1987) friction-factor equation) to 0 for a tube with high roughness height. Equation (5) provides a correct asymptotic trend to the bundle correction factor (i.e., no correction is applied to the friction factor for tubes at high Reynolds numbers where 'b' becomes 0). Since the friction factor is affected by the correction factor for geometry and the exponent (which in turn depends on the friction factor), an iterative procedure is required.

The correction factor, $K_{ecc.}$, accounts for the eccentricity effect of the bundle inside a pressure

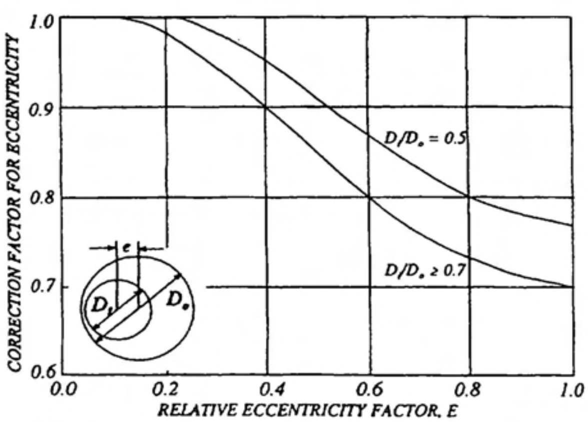

Figure 2: The Idelchik correction factor for the eccentricity effect.

tube, and is calculated with the Idelchik equation (1994) for annuli. Figure 2 presents the Idelchik correction factor for the eccentricity effect. To extend to a rough channel, the same modification as Equation (5) is introduced:

$$K_{ecc.} = 1 - (1 - K_{ecc.,\,Idelchik})\,\frac{b}{0.311} \qquad (7)$$

The relative eccentricity factor is defined as

$$E = \frac{2\,e}{D_o - D_i} \qquad (8)$$

where e is the radial distance between centres of the inner and the outer tubes (in metres).

The Idelchik methodology is presented in terms of both the outer and inner diameter of tubes in the annuli. In CANDU fuel-channel analyses, the pressure tube (or the flow tube) is considered as the outer tube. A characteristic inner-tube diameter of the annuli is introduced to represent the surface of all elements in the bundle with a single equivalent surface. This characteristic diameter does not affect the hydraulic-equivalent diameter used in the pressure-drop calculations (such as the D'Arcy equation). Three different definitions have been examined:

(1) based on the traditional definition of hydraulic-equivalent diameter in annuli,
(2) based on the equivalent area occupied by all elements, and
(3) based on the weighted-average pitch-circle-diameter values of all rings.

The first two approaches, based on the hydraulic-equivalent diameter and the total occupied area of all elements, cannot be used to account for a variation in pitch to rod-diameter ratio, which is a primary factor in bundle friction factor (Idelchik 1994). Therefore, the approach based on the weighted-average pitch-circle diameter is used to evaluate the characteristic inner-tube diameter for a CANDU-type bundle. The characteristic inner-tube diameter is expressed as

$$D_i = D_{rod} + \frac{6\,D_{ir} + 12\,D_{mr} + 18\,D_{or}}{36} \tag{9}$$

where D_{ir}, D_{mr} and D_{or} are the pitch-circle-diameter values from the centre of the bundle to the centre of the element in the inner ring, middle ring and outer ring, respectively, in metres.

2.2 Single-Phase Pressure Drops over Bundle Junction, Spacers and Bearing-Pad Planes

The single-phase local pressure drops over bundle junction, spacers and bearing-pad planes are calculated using

$$\Delta P_{local} = K_{local}\,\frac{G^2}{2\,\rho_l} \tag{10}$$

This equation is derived for blockages with small thickness, and hence the frictional pressure drop over the blockage is negligible.

2.2.1 Loss Coefficient for Bundle Junction

The loss coefficient over the junction of two aligned CANDU-type bundles is assumed to consist of two components: impact loss caused by webs of the endplate and separation loss over two planes of rod. It is expressed as

$$K_{junction} = C_{ecc.}\,(K_{imp.} + K_{sep.}) \tag{11}$$

where $C_{ecc.}$ is the correction factor for eccentricity effect.

Impact Loss: The impact loss coefficient is calculated with

$$K_{imp} = a_1\left(\tan\left(\left(\frac{A_{ob}}{A_f}\right)^2 \frac{\pi}{2}\right)\right)^{b_1} \tag{12}$$

where A_{ob} is the blockage area in m^2, A_f is the flow area in m^2, and A_{ob}/A_f is often referred to as the blockage-area ratio. The constants, a_1 and b_1, are optimized using data of Salcudean and Leung (1988), and are shown in Table 1 for various blockage locations (Figure 3). Due to the lack of data for large flow blockages, the application of Equation (12) is limited to blockage-area ratios of less than 45%. The selection of the appropriate correlation depends strongly on the distribution of blockages in the channel.

Rod Separation Loss: A rod separation can be characterized as a sudden expansion followed rapidly by a sudden contraction. Therefore, the loss coefficient over the rod separation plane is written as

$$K_{sep.} = C_\delta\,(K_{exp.} + K_{cont.}) \tag{13}$$

where C_δ is a correction factor for the gap size.

Sudden Expansion: The loss coefficient for a sudden expansion is presented by Idelchik (1994) as

Table 1: Loss coefficients of various obstructions (Salcudean and Leung 1988).

	Vertical channel		Horizontal channel		Constants in Equation (12)	
Blockage-area ratio	25%	40%	25%	40%	a_1	b_1
Central	0.9	2.17	0.91	2.19	7.59	0.9175
Peripheral	0.44	1.88	0.48	1.9	14.038	1.4748
Central segment	0.75	2.15	0.75	2.13	9.3797	1.088
Peripheral segment	0.7	2.05	0.71	2.03	11.859	1.2874

$$K_{exp.} = \left(1 - \frac{A_f}{A_o}\right)^2 \quad \textbf{(14)}$$

The total area of the flow tube is used as the expanded area, A_o, because it is the immediate area behind the rod, and corresponds generally to the high turbulence-generation zone. The small area covered by the spigot at the end plug is neglected for simplicity. The area of the endplate is not considered, because most of it has been included in the impact-loss calculation, which includes the losses due to contraction and expansion over the blocking web. Other areas of the endplate are behind the rod and are assumed to have no impact on turbulence generation.

Sudden Contraction: Similarly, the loss coefficient for a sudden contraction is presented by Idelchik (1994) as

$$K_{cont.} = 0.5\left(1 - \frac{A_f}{A_o}\right)^{3/4} \quad \textbf{(15)}$$

Gap Effect: The correction factor for the gap effect, C_δ, is introduced to account for the effect of gap size on the loss coefficient. It has the asymptotic values of 0 for the no-gap case, and 1 for an infinitively large gap. Based on data obtained in a bundle-separation test (CGE unpublished report), the correction factor for gap effect, C_δ, can be expressed as

$$C_\delta = 1 - \exp\left(-\left(0.8476\frac{\delta}{D_{rod}}\right)^{1.1687}\right) \quad \textbf{(16)}$$

Blockage-Eccentricity Effect: Idelchik (1994) showed that the correction factor for blockage-eccentricity effect is expressed as

$$C_{ecc.} = (1 - E')^{3/m} \quad \textbf{(17)}$$

where E' is the ratio of radial distance (from the centre of the channel to the centre of the blockage) to the hydraulic radius of the channel, and m is the exponent value in the power law for a universal-velocity profile. Based on data presented by Idelchik (1994), the exponent 'm' can be represented by the following equation:

$$m = 1.803\ \log(Re) - 1.586 \quad \textbf{(18)}$$

2.2.2 Loss Coefficient for Spacer Plane

The pressure drop over the spacer plane of a CANDU-type bundle is caused mainly by the impact loss when the flow passes over the spacers and bearing pads. It depends on the impact area of these blockages. In addition, the rounding of the leading and trailing edges of the spacer and bearing pad as well as the tilting from the flow direction (about 15° in a 37-element bundle) affect the pressure drop. The loss coefficient for the spacer plane is expressed as

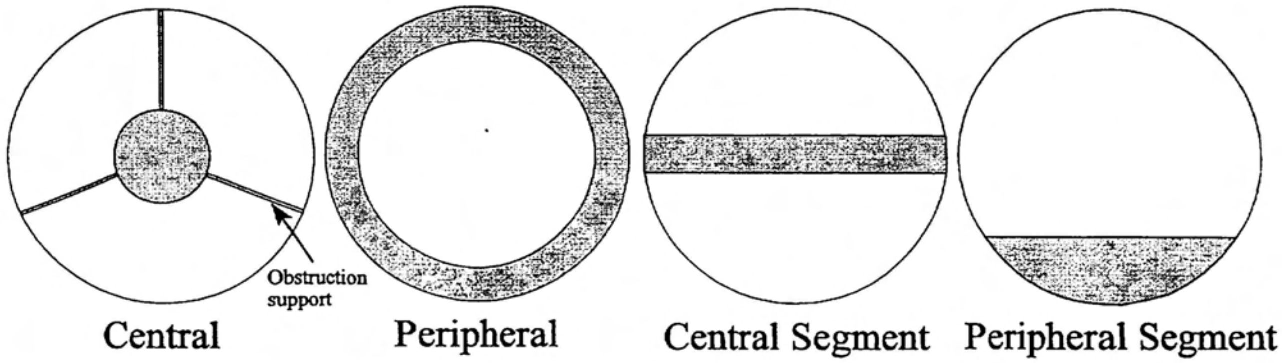

Figure 3: Types of obstruction tested by Salcudean and Leung (1988).

$$K_{spacer} = C_{ecc.} C_{shape} K_{imp.} \quad (19)$$

where $K_{imp.}$ is the impact loss coefficient, $C_{ecc.}$ is the correction factor for overall blockage eccentricity within the pressure tube, and C_{shape} is the correction factor for shape and tilt. The correction factor for blockage eccentricity is calculated with Equation (17).

Impact Loss: The impact loss over the spacer plane is calculated with Equation (12). The flow-impact area of the blockage is calculated using the dimensions of the spacers and bearing pad. It is expressed as

$$A_{ob} = \sum_{j=1}^{M} \left(\sum_{i=1}^{N} (A_{sp_j,f} \cos\theta)_i + \sum_{i=1}^{N} (A_{sp_j,s} \sin\theta)_i \right) + \sum_{i=1}^{K} (A_{bp,f})_i \quad (20)$$

where θ is the spacer skew angle from the flow direction (about 15° for a 37-element bundle), N is the number of spacers of the same type, M is the number of different types of spacer, and K is the number of bearing pads at the middle plane. The subscript "sp" corresponds to the spacer, "bp" refers to the bearing pad, and "f" and "s" correspond to the frontal and side area of the spacer, respectively.

Idelchik (1994) showed the strong effect of the shape of the leading and trailing edges of a blockage on pressure drop. A reduction of 24% in pressure drop is shown by simply rounding the leading and trailing edges of the rod. The skewness of the blockage to the flow direction also affects the pressure drop. For a plate perpendicular to the flow, the drag coefficient is 1.16. This factor affects both the spacer and the bearing pad. The combined correction factor for the shape and skewness of the blockage is calculated using

$$C_{shape} = \frac{C_{edge}}{A_{ob}} \sum_{j=1}^{M} \sum_{i=1}^{N} (A_{sp,f} \cos\theta)_{i,j} + \frac{C_{skew,sp}}{A_{ob}} \sum_{j=1}^{M} \sum_{i=1}^{N} (A_{sp,s} \sin\theta)_{i,j} + \frac{C_{skew,bp}}{A_{ob}} \sum_{i=1}^{K} (A_{bp,f})_i \quad (21)$$

2.2.3 Loss Coefficient for Bearing-Pad Plane

The pressure drop over the bearing-pad plane of a CANDU-type bundle is calculated using the same methodology as for the spacer plane.

2.3 Single-Phase Pressure Drop due to Acceleration

The single-phase pressure drop due to acceleration is calculated from

$$\Delta P_{sp,acc.} = G^2 \Delta v_l = G^2 \Delta \left(\frac{1}{\rho_l} \right) \quad (22)$$

where v_l is the liquid specific volume in $m^3 \cdot kg^{-1}$.

3. VALIDATION OF THE GENERALIZED PREDICTION METHOD

The generalized prediction method for pressure drop has been validated with three sets of data obtained in several strings of CANDU bundles:

(1) friction factor and loss coefficients (for bundle junction and midplane spacers and bearing pads) of a string of simulated 4-element bundles in low-pressure water flow,
(2) friction factor and loss coefficients (for bundle junction and midplane spacers and bearing pads) of a string of 37-element bundles in high-pressure Freon flow, and
(3) friction factor and loss coefficient for bundle junction of three strings of 37-element bundles in high-pressure water flow.

However, only the comparison against the data obtained at Chalk River Laboratories (CRL) with the 37-element bundle string in Freon flow (Hameed, AECL unpublished report) is presented here.

The test bundle consists of 37 rods, each of which comprises a Zircaloy tube containing uranium pellets. Both ends of the rod are covered with the end plugs. These rods are connected to two endplates (one at each end), and are separated by spacers. There are two sizes of spacer, to accommodate the differences in gap size between elements. Figure 4 shows schematically the cross-sectional bundle configuration.

3.1 Friction Factor

The friction factor is calculated with the equivalent, cross-sectional average, surface-roughness height using

$$\varepsilon_{channel} = \frac{37\ \varepsilon_{rod} D_{rod} + \varepsilon_{tube} D_{tube}}{37\ D_{rod} + D_{tube}} \tag{23}$$

where D_{rod} and ε_{rod} are the outer diameter and measured surface-roughness height, respectively, of the element in metres, and D_{tube} and ε_{tube} are the inner diameter and measured surface-roughness height, respectively, of the flow tube in metres.

Figure 5 compares the calculated and experimental friction factor over the range of Reynolds numbers. The predictions of the proposed method agree very well with the data over the full range of Reynolds numbers. Overall, the present method predicts the data with an average error of -0.33% and a root-mean-square (rms) error of 3.79%. The prediction accuracy is much better than the Colebrook equation (average error of -3.49% and rms error of 5.23%), and the Blasius equation (average error of -9.65% and rms error of 11.16%).

The average error is defined as

$$Average\ Error = \frac{1}{N}\sum_{i=1}^{N} (Error)_i \tag{24}$$

and the rms error is

$$Rms\ Error = \sqrt{\frac{1}{N}\sum_{i=1}^{N} (Error)_i^2} \tag{25}$$

where

$$Error = \frac{Pred.\,Value - Expt.\,Value}{Expt.\,Value} \tag{26}$$

3.2 Loss Coefficient for Bundle Junction

The loss coefficient for the junction of two aligned Bruce bundles is calculated using Equation (11). Since the blockages are distributed uniformly across the bundle, the blockages are assumed to have the same

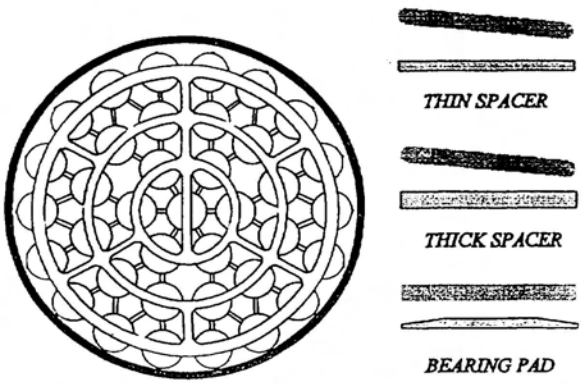

Figure 4: Schematic diagram of the 37-element bundle.

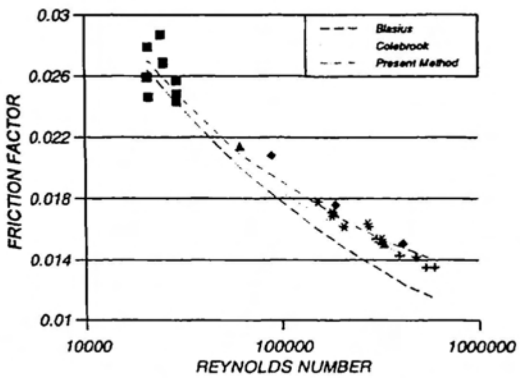

Figure 5: Comparison of predicted and experimental friction factors for 37-rod bundles.

eccentricity as the bundle, and are distributed evenly across the bundle and resemble roughly a central-segment obstruction. Therefore, the coefficients for the central-segment obstruction (Table 1) is used to determine the impact loss coefficient for the exposed end-plate webs in a 37-element bundle.

Based on the proposed method, the calculated loss coefficients for the junction plane of two aligned Bruce bundles vary from 0.4411 to 0.4436 over the range of Reynolds numbers from 10 000 to 1 000 000. They are smaller than the mean value of all data, which is 0.47, but appear to agree with the lower-bound value (about 0.43). Figure 6 shows the comparison between predictions and measurements.

An improvement to the agreement is observed if the impact loss coefficient is evaluated with the mean value of the central and the central-segment obstructions. The calculated loss coefficients vary from 0.4925 to 0.4954 over the same range of Reynolds numbers.

3.3 Loss Coefficient for Spacer Plane

The loss coefficient for the spacer plane of the 37-rod bundle is calculated using Equation (19). Since the bundle eccentricity is uniform throughout the bundle string (in an uncrept channel), the same correction factor for bundle eccentricity, as calculated for the junction plane is applied. All blockages are in the small gap between two elements, where the flow velocity is often low. Therefore, the coefficients for the peripheral obstruction (Table 1) are used to calculate the impact loss coefficient.

The correction factor for shape, C_{edge}, is 0.76, as recommended by Idelchik (1994). The correction factor for skewness, $C_{skew, sp}$, is approximated with the drag coefficients presented by Idelchik (1994) and is 0.065 for a 15° tilt angle to the flow. Similarly, the correction factor for skewness, $C_{skew, bp}$, is 0.38 at a 30° tilt angle to the leading edge of the bearing pad.

The calculated loss coefficient is 0.112 for the spacer plane of the 37-rod bundle. This agrees closely with the mean value of the data as presented in Figure 7.

3.4 Loss Coefficient for Bearing-Pad Plane

The loss coefficient for the bearing-pad plane was not measured, because the pressure drop over the bearing pads is much smaller than the uncertainty level of the measurements. Nevertheless, it is calculated in this study for completeness. The impact loss coefficient is calculated with the coefficient for a peripheral obstruction. The correction factor for skewness, $C_{skew, bp}$ is 0.38. Based on this information, the calculated loss coefficient is only $1.25 \cdot 10^{-5}$ for a plane of staggered bearing pads (i.e., nine bearing pads in a 37-rod bundle). Although the loss coefficient for

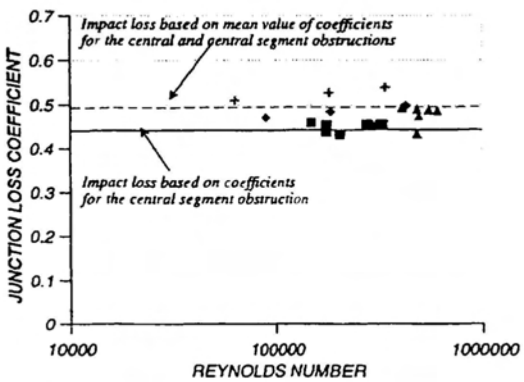

Figure 6: Comparison of predicted and measured loss coefficients for aligned 37-rod bundle junction.

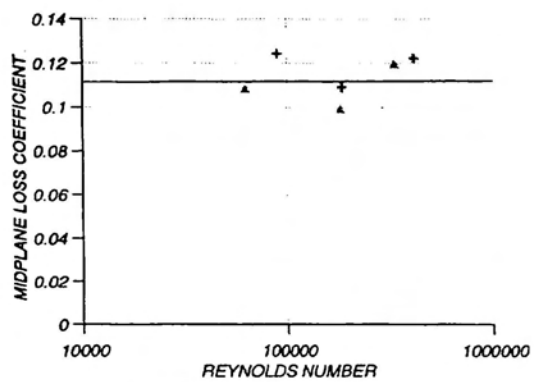

Figure 7: Comparison of predicted and measured loss coefficients at the spacer plane.

the bearing-pad plane appears to be negligible based on the cross-sectional average value, it can be a significant factor to the local flow distribution at the vicinity of a bearing pad. This has been observed from the CRL experiments: a measurement probe located at the outer subchannel showed a pressure change over the bearing pad, while another probe located at the inner subchannel did not detect the presence of bearing pads at all.

4. ASSESSMENT OF THE PREDICTION METHOD WITH DATA OF A FULL-SCALE BUNDLE STRING

The prediction capability of the proposed generalized method is assessed with the single-phase pressure-drop data obtained over a full-scale bundle string inside both the reference and crept channels at Stern Laboratories (SL). This assessment focuses mainly on the data of adiabatic flow, since the effect of heating on pressure drop has not been examined.

The SL bundle string simulated closely twelve aligned 37-element Bruce-type fuel bundles. Both the axial and radial heat-flux distributions at the fuel bundle were simulated by using tubes with varying wall thicknesses. Loop conditions at both inlet and outlet ends of the bundle string were monitored with differential-pressure cells and Chromel-Alumel (K-Type) thermocouples. In addition, pressure taps were installed at various locations along the bundle string to obtain pressure-drop data. Spring-loaded thermocouples mounted on sliding carriers were installed inside all elements of the five downstream bundles. They were moved axially and radially to obtain surface-temperature measurements on various locations of each element. Besides the tests with an uncrept channel, experiments were also carried out using ceramic liners of varying diametral values along the bundle string, to simulate a crept channel. Two axial diametral profiles were used to simulate 3.3% and 5.1% maximum creep values.

Table 2: Prediction accuracy for channel pressure drop over a full-scale bundle string.

Data series (% of dia. creep)	No. of data	Error (%)		Error range (%)	
		Avg.	Rms.	from	to
R1 (0%)	42	-3.18	3.671	-5.51	1.725
R2 (0%)	38	0.496	1.318	-2.91	2.559
M (0%)	10	0.615	0.876	-0.36	1.506
U (0%)	40	-0.66	1.061	-2.86	0.946
R3 (0%)	10	-0.99	1.735	-3.16	0.931
C1 (3.3%)	37	-0.4	1.524	-4.5	1.931
C2 (5.1%)	109	-0.1	1.26	-5.2	1.469
All data	286	-0.6	1.845	-5.51	2.559

The overall bundle pressure drop is calculated with the assumption that the test string simulates closely the Bruce bundle configuration. Therefore, the same bundle dimensions as in the comparison against the CRL data are used, except for the flow-tube diameter. The flow tube of the SL test is slightly larger than that in the CRL test, and has an inside diameter of 103.86 mm.

The frictional pressure drop is calculated with the measured roughness-height values of the surface of all elements and the ceramic flow tube. For comparison purposes, the impact loss coefficient at the bundle junction plane is calculated with the average value for the central and central-segment obstructions, which has been shown to agree better with the CRL data.

Table 2 lists the prediction accuracy of the generalized method for the overall bundle-string

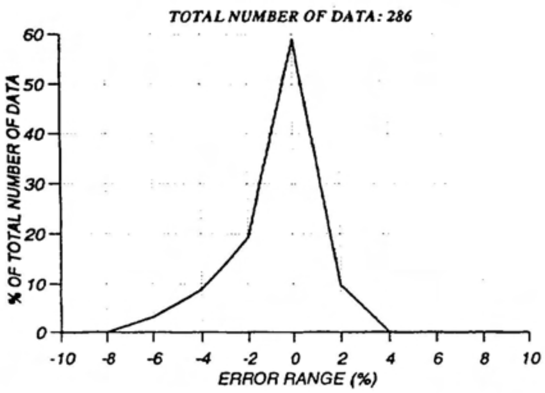

Figure 8: Distribution of data within a 2% range of prediction error.

pressure drop in various series. An excellent agreement is shown between the predictions and the measurements, with an overall average error of -0.6% and an rms error of 1.85%. Except for the R1 series and one point in the C2 series, all data are predicted within the ±5% error range. The distribution of data over various error ranges is shown in Figure 8. A close examination of data in the R1 series shows that data of large prediction error were obtained on a single date of testing. The prediction accuracy for this series improves significantly when the suspect data are excluded: it results in an average error of -0.102% and an rms error of 1.776 for six data points in the R1 series, and all of them are within the ±5% error range.

5. CONCLUSIONS AND FINAL REMARKS

- A generalised prediction method has been developed for single-phase pressure drop in a CANDU-type bundle string.
- The predictions of the generalised method for various pressure-drop components have been compared against experimental data obtained with several strings of CANDU-type bundles having a 4-rod and a 37-rod bundle configuration. Good agreements between predictions and measurements were observed.
- The methodology can be extended to misaligned bundle configurations. This will ensure that the generalised prediction method is applicable for actual fuel-channel analysis.

6. REFERENCES

Bhatti, M.S. and Shah, R.K., "Turbulent and transition flow convective heat transfer in ducts", *Handbook of single-Phase Convective Heat Transfer* (Editors: Kakaç, S., Shah, R.K. and Aung, W.), John Wiley and Sons, Inc., 1987.

Courtaud, M., Ricque, R. and Martinet, B., "Etude des pertes de charge dans des conduites circulaires contenant un faisceau de barreaux", *Chem. Eng. Sci.*, Vol. 21, pp. 881-893, 1966.

Idelchik, I.E., *Handbook of Hydraulic Resistance*, CRC Press Inc., 3rd Edition, 1994.

Le Tourneau, B.W., Grimble, R.E. and Zerbe, J.E., "Pressure drop for parallel flow through rod bundles", Trans. ASME, pp. 1751-1758, November, 1957.

Malak, J., Hejna, J. and Schmid, J., "Pressure losses and heat transfer in non-circular channels with hydraulically smooth walls", *Int. J. Heat Mass Transfer*, Vol. 18, pp. 139-149, 1975.

Rehme, K., "Simple method of predicting friction factors of turbulent flow in non-circular channels", *Int. J. Heat Mass Transfer*, Vol. 16, pp. 933-950, 1973.

Salcudean, M.E. and Leung, L.K.H., "Pressure drop due to flow obstruction", *Nuclear Engineering Design*, Vol. 105, pp. 349-362, 1988.

7. ACKNOWLEDGEMENTS

The authors would like to thank J. Schenk for his assistance in calculating the flow blockage area, A. Hameed for providing the Freon data, D.C. Groeneveld for his comments, and test engineers at Ontario Hydro and Stern Laboratories for providing data from the recent full-scale bundle tests. Financial support from Working Party 12 of the CANDU Owners Group (COG) is appreciated.